International Research Journal of Education and Technology
Peer Reviewed Journal
ISSN 2581-7795

NON ISOLATED MULTIPORT DC-DC CONVERTER

DR.SATHISHKUMAR.S(AP SELECTION GRADE,DEPT OF EEE,BANNARI AMMAN INSTITUTE OF TECHNOLOGY,SATHYAMANGALAM)

MOHNIKA T K (DEPARTMENT = ELECTRICAL AND ELECTRONICS ENGINEERING)

NANTHITHA PARKAVI J R (DEPARTMENT = ELECTRICAL AND ELECTRONICS ENGINEERING)

DIVYASHREE R (DEPARTMENT = ELECTRICAL AND ELECTRONICS ENGINEERING)

JABEZ DURAI S (DEPARTMENT = ELECTRICAL AND ELECTRONICS ENGINEERING)

Abstract - This paper introduces a new type of DC-DC converter that combines multiple energy sources (like solar panels and batteries) into one system without using transformers. This design is smaller, simpler, and cheaper than traditional converters. It uses a special circuit that can both increase and decrease voltage to control the power flow between the sources. A specific control method (PWM) is used to keep the output voltage stable and the system efficient. The design was tested using computer simulations and a physical prototype. The results showed high efficiency (92% in simulation, 89% in hardware) and stable voltage even when the load changed. This converter is well-suited for use in renewable energy systems and electric vehicles because of its small size and good performance.

1. Introduction

With the increasing adoption of renewable energy and electric vehicles, there's a greater demand for power conversion systems that are both efficient and adaptable. In energy systems that combine various sources like solar panels, fuel cells, and batteries, multiport DC-DC converters are essential for managing power flow and maintaining a stable output.

Conventional converters use transformers to isolate the circuits, but this makes them larger, more expensive, and more complicated. Non-isolated multiport DC-DC converters (NIMPCs) remove the need for transformers, resulting in a more compact design, lower costs, and simpler control.

This paper explores how a non-isolated multiport DC-DC converter can effectively combine power from multiple sources into a single output, while also keeping the system small and affordable.

Objectives:

The study aims to:

- Create a compact NIMC suitable for renewable energy applications.
- Use PWM-based control methods to dynamically regulate the output voltage.
- Test the system's performance through both simulations and a physical prototype, then compare the results.

Literature Review:

Several studies have explored the design and control of multiport DC-DC converters:

- **A. Sharma et al.** (2023) designed an isolated multiport converter for hybrid energy systems, achieving high efficiency but introducing transformer-related complexity.
- **B. Kumar et al.** (2022) proposed a non-isolated converter for EV charging, highlighting the benefits of compact design and reduced cost.
- **C. Lee et al.** (2021) developed a PWM-controlled bidirectional DC-DC converter, improving load regulation and dynamic response.

While these studies advanced the field, **gaps** remain in optimizing non-isolated converters for higher efficiency and reduced switching losses. This paper addresses these gaps by designing a **bidirectional NIMPC** using **PWM control** to enhance voltage stability and power distribution.

International Research Journal of Education and Technology
Peer Reviewed Journal
ISSN 2581-7795

2. Methodology

The methodology is broken down into system design, simulation, and hardware implementation.

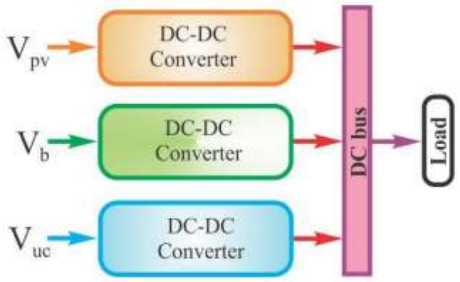

2.1 Block Explanation

Voltage Sensor: This sensor is responsible for measuring the voltage of the battery. It detects the electrical potential difference between two points in the battery system and sends this data to the IoT platform for monitoring and analysis.

Temperature Sensor: The temperature sensor monitors the temperature of the battery. It provides real-time temperature data to the IoT system. If the temperature exceeds a predefined threshold, indicating a potential overheating issue, the system triggers a buzzer alert and displays a warning message on the LCD screen.

Fire Sensor: This sensor is crucial for safety. It detects the presence of fire or extreme heat near the battery. If a fire is detected, the sensor activates an alarm to alert nearby individuals and initiates appropriate safety protocols.

IoT Platform: The IoT platform serves as the central hub for data collection, processing, and analysis. It receives data from various sensors such as voltage and temperature sensors, processes this data, and provides insights into the battery's health and performance. It also facilitates remote monitoring and control of the battery system.

Buzzer: The buzzer is an audible alarm device that is activated in case of critical events such as overheating or fire detection. It alerts nearby individuals to potential safety hazards associated with the battery.

LCD Display: The LCD display provides a user interface for visualizing important information such as battery voltage, temperature, and alarm notifications. It allows users to quickly assess the status of the battery system without accessing the IoT platform.

2.2 Circuit Diagram

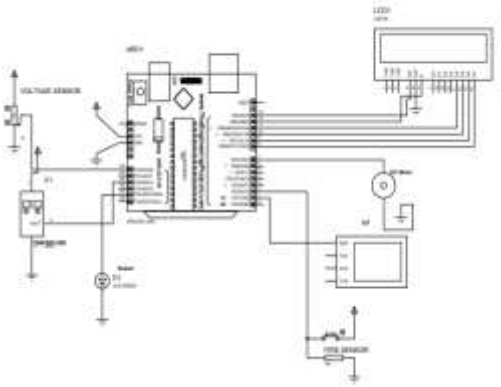

A. System Design: The NIMPC was designed to combine power from a 24V solar panel and a 48V battery into a single load. The design features a bidirectional buck-boost converter, which allows power to flow in both directions between the sources and the load. MOSFETs (IRF540) are used as switching devices, operating at 50 kHz. A PWM-based control system is implemented to adjust the duty cycles of the switches and maintain a stable output voltage.

B. Simulation: The system was simulated using MATLAB Simulink. The simulation parameters included an input voltage range of 24V to 48V, an output voltage regulated at 36V, and a switching frequency of 50 kHz.

C. Hardware Implementation: The hardware prototype uses key components such as MOSFETs (IRF540) for fast switching, 100 µH inductors for voltage regulation, an Arduino Uno microcontroller to generate PWM signals, and 1000 µF capacitors to reduce output voltage fluctuations. The PCB layout was designed using EAGLE software to minimize switching losses and improve heat dissipation.

International Research Journal of Education and Technology
Peer Reviewed Journal
ISSN 2581-7795

Result:

A. Simulation Results

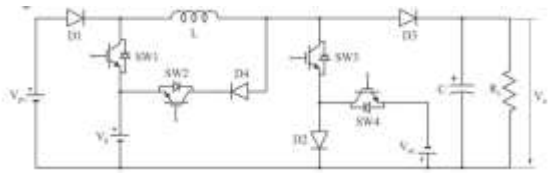

Fig.2 The structure of a four-port non-isolated DC-DC converter.

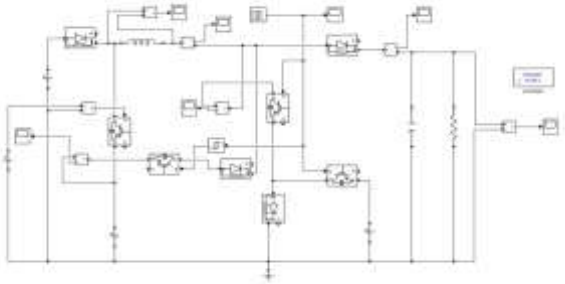

Fig.3 The MATLAB/SIMULINK model of a four-port non-isolated DC-DC converter.

Operating Modes

The converter operates in different modes depending on which switches (static contactors) are on or off, controlling the flow of energy. There are five main operating modes:

- **Mode 1:** The solar panel (Vpv) directly powers the load (represented by a resistor Rs).
- **Mode 2:** The battery supplies power to the load.
- **Mode 3:** Both the solar panel and the ultracapacitor supply power to the load.
- **Mode 4:** The battery and the ultracapacitor jointly supply power to the load.
- **Mode 5:** The battery is charged by the solar panel.

Mode 1 Details:

In this mode, the load receives power from the solar panel. Whether the static contactors are blocking (OFF) or conducting (ON) determines how the converter operates in each mode.

- M 1. Figure 4 shows the Conduction State (I) in full. The inductor L draws current from the solar panel

when switches SW3, D1, and D2 are turned on, and this current rises linearly.

$$\frac{di_L}{dt} = \frac{V_{pv}}{L} \quad (1)$$

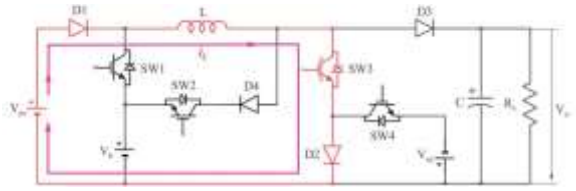

.Fig. 4: Mode 1, state I

Fig. 5 describes Mode 1: Blocking State (II). In this condition, diodes D1 and D3 are ON and switch SW3 is OFF. The load (Rs) is charged by current flowing from the inductor (L) and the solar panel (Vpv). There is a formula that determines how quickly the inductor current drops.

$$\frac{di_L}{dt} = \frac{V_{pv} - V_o}{L} \quad (2)$$

Assuming the circuit operates in continuous current mode, the volt-second balance theorem applied to inductor L gives the equation

$$V_L = V_{pv} - V_o(1 - D_c) = 0 \quad (3)$$

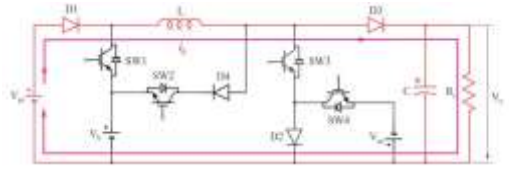

Fig.5: Mode I, State II.

Here, Dc represents the duty cycle $D_c = \frac{t_{on}}{t_{on} + t_{off}} \cdot 100$ of switch SW3, which is 25% in this case. Based on this, a further equation is derived

$$V_o = \frac{V_{pv}}{1 - D_c} \quad (4)$$

International Research Journal of Education and Technology
Peer Reviewed Journal
ISSN 2581-7795

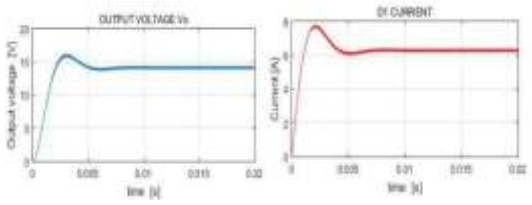

Fig.6: voltage variation over time from the converter's output on charge and current via diode D1.

The voltage at the load stabilizes at 14V, and the current drawn is 6.3A, when the solar panel voltage (Vpv) is 12V and the duty cycle (Dc) for switch SW3 is 25%. Simulations demonstrate that, as anticipated, the output voltage rises proportionately with the duty cycle (Dc) given a constant input voltage and load. Fig. 7 displays the characteristic signals for operating mode 1.

Mode 2: The battery powers the load in this working mode (Vb = 12V).

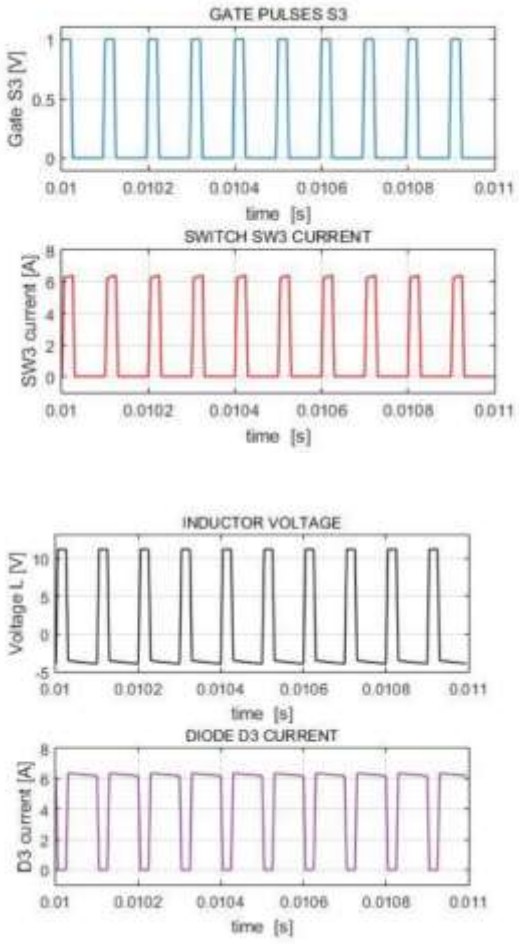

Fig. 7: The Operating Mode 1

Mode 2 signals (shown in Fig. 8) are as follows: The battery that provides the charge

- State I: Diode D2, switches SW1, and SW3 are all turned on. Current is drawn from the battery by inductor L, and it rises linearly:

$$\frac{di_L}{dt} = \frac{V_b}{L} \quad (5)$$

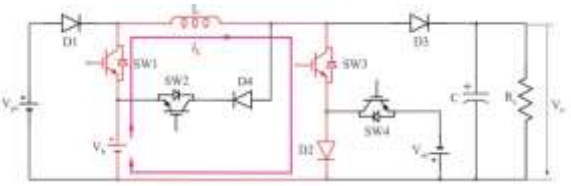

Fig 8: Mode 2, State I

State II (shown in Fig. 9): The battery provides the charge through inductor L, and switches SW1 and diode D3 are turned on. A particular equation determines the pace at which the current drops:

$$\frac{di_L}{dt} = \frac{V_b - V_o}{L} . \quad (6)$$

The volt-second balance condition for inductor L is also provided

$$V_o = \frac{Vb}{1 - D_c} . \quad (7)$$

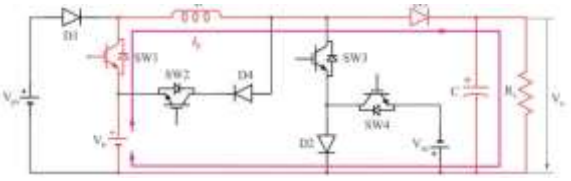

Fig 9: Mode 2, State II

Control Circuitry Explanation:

In Mode 2, switch SW1 remains ON in both states of switch SW3. To ensure this, the gate of SW1 is continuously polarized by a voltage source (Vpol). 8This voltage is maintained as long as it exceeds the base-emitter voltage required to keep the IGBT transistor (SW1) fully open. A value of Vpol = 1V was deemed sufficient.

International Research Journal of Education and Technology
Peer Reviewed Journal
ISSN 2581-7795

With a battery voltage (Vb) of 12V and a duty cycle of 25%, the output voltage and absorbed current values are similar to those in Fig. 6 (not provided).

The voltage source Vpol is not shown in the main circuit diagrams because it is part of the control and command structure, not the power circuit itself. However, in the MATLAB/Simulink model, the pulse generator, relay inverter (which controls the static contactors and allows modification of the duty cycle Dc), and the polarization voltage Vpol for SW1 are included. This approach allows a consistent power circuit structure to be used across all operating modes.

Switching between operating modes is achieved by changing the value of Vpol. It is set to 1V only for

Modes 2 and 4, and to 0V (SW1 is OFF) for all other modes.

In summary, Vpol, the pulse generator, and the relay are part of the control circuit and not part of the power circuit, which is why they are not depicted in Figs. 1 and 2. Fig. 10 shows the characteristic signals for this operating sequence.

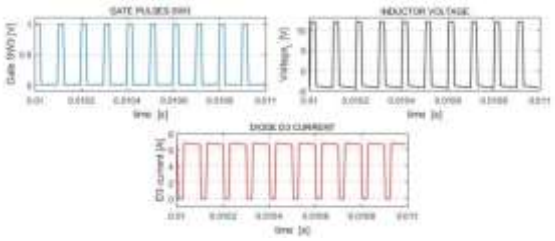

Fig. 10. Modului 2's distinctive signals.

Mode 3: Solar Panel and Ultracapacitor Supplying the Charge

This mode is employed when the output voltage (V0) decreases as a result of the solar panel voltage (Vpv) falling below a predetermined threshold. The solar panel is still the main energy source, but an ultracapacitor is added to the circuit to make up for this voltage loss.

- State I (shown in Fig. 11): Switches SW3, SW4, and diodes D1 are all on. As the circuit shuts off, energy is absorbed by inductor L. A particular equation provides the rate at which the current flows through inductor L.

$$\frac{di_L}{dt} = \frac{V_{pv} + V_{uc}}{L} \quad (8)$$

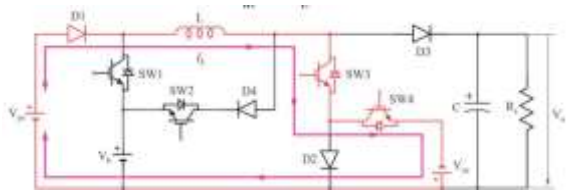

Fig.11:. Mode 3, State I

State II: Diodes D1 and D3 are turned on (seen in Fig. 12). After the collected energy is transmitted to the load, a certain equation governs how the inductor current varies.

$$\frac{di_L}{dt} = \frac{V_{pv} - V_o}{L} \quad (9)$$

Applying the volt-second balance condition for inductor L results in an equation

$$V_L = V_{pv} + D_c \cdot V_{uc} - V_o(1 - D_c) = 0 \quad (10)$$

which can be rearranged to solve for another term

$$V_o = \frac{V_{pv} + D_c \cdot V_{uc}}{1 - D_c} \quad (11)$$

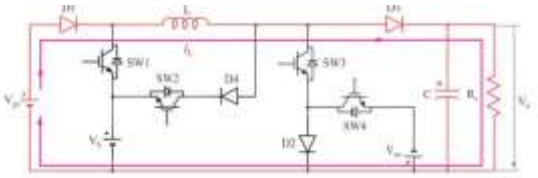

Fig.12:. Mode 3, State II.

The characteristic signals for this operating mode are displayed in Fig. 13.

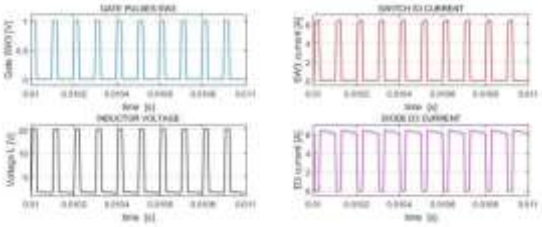

Fig 13. Modului 3's distinctive signals

The output voltage used in Fig. 13 was the same as that in Fig. 6: Vpv = 9 V, Vuc (ultracapacitor voltage) = 12 V, and Vpol = 0 (due to SW1 being blocked).

Mode 4: Battery and Ultracapacitor Supplying the Charge

In this mode, the ultracapacitor assists the battery in the same way it assisted the solar panel in Mode 3.

- State I(Fig 14): Switches SW1, SW3, and SW4 are ON.

International Research Journal of Education and Technology
Peer Reviewed Journal
ISSN 2581-7795

voltage) = 12 V, and Vpol = 0 (due to SW1 being blocked).

Mode 4: Battery and Ultracapacitor Supplying the Charge

In this mode, the ultracapacitor assists the battery in the same way it assisted the solar panel in Mode 3.

- State I(Fig 14): Switches SW1, SW3, and SW4 are ON.

Fig. 14. Mode 4,State 1.

- State II (Fig. 15): Diode D3 and switches SW1 are turned on.

With the exception of substituting the battery voltage (Vb) for the solar panel voltage (Vpv), the inductor current equations are identical to those in Mode 3 (equations 8 and 9 in the original article). A similar outcome is obtained by applying the flow conservation theorem.

$$V_o = \frac{V_b + D_c \cdot V_{BC}}{1 - D_c} \quad (12)$$

With the exception of the battery (Vb) replacing the solar panel (Vpv), the outcomes are the same as those in operating mode 3.

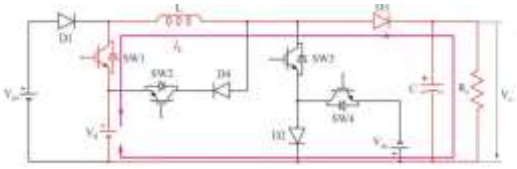

Fig 15:Mode 4, State II.

Fig. 16 shows the sample signals for operating mode 4.

Mode 5: Solar Panel Charging of Batteries

In this mode, the solar panel charges the battery (Vpv). This happens while the PV panels are producing energy and the car is not moving. The

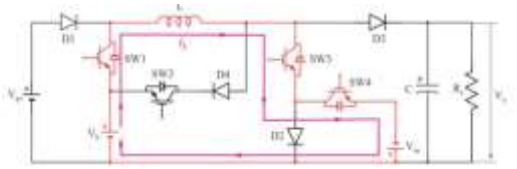

The battery is charged using the extra energy produced by the solar panels.

State I: Diodes D1 and D2 are turned on, as are switches SW3.

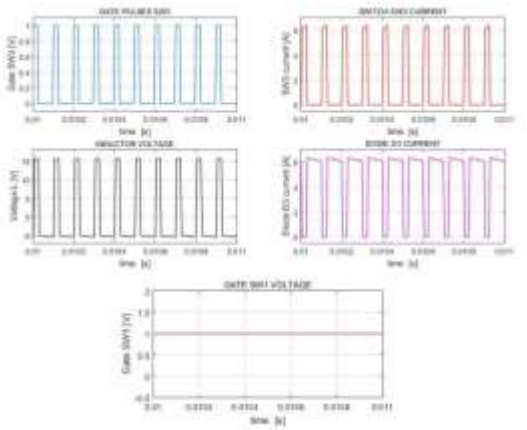

Fig.16.Modului4'sdistinctivesignals

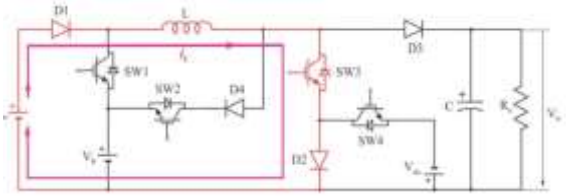

Fig.17:. Mode 5, State I.

- State II (Fig. 18): Diodes D1, D4, and SW2 are all turned on. Switches SW2 and SW3 are never on simultaneously since their conduction states are complementary.

The voltage at the battery terminals in a steady state is calculated using a particular calculation that applies the flow conservation theorem.

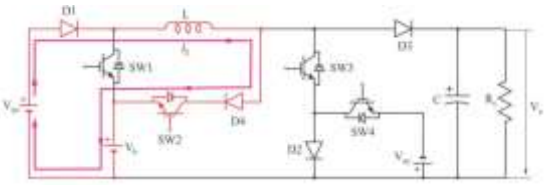

Fig 18:Mode 5, State II..

Figure 19 displays the typical parameters' temporal evolution for this operating mode.

International Research Journal of Education and Technology
Peer Reviewed Journal
ISSN 2581-7795

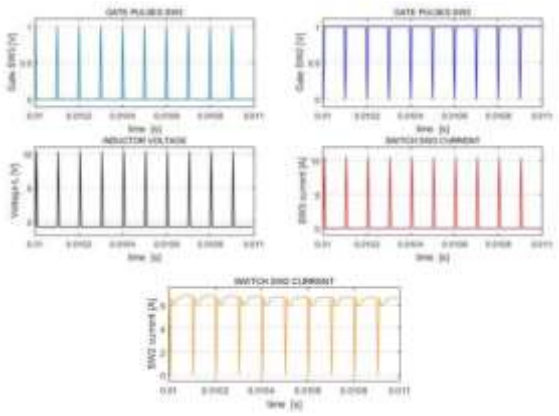

Fig. 19: Modului 5's characteristic signals

As shown in Fig. 19, the simulation results for Mode 5 were obtained using a duty cycle (Dc) of 5% for switch SW3, a solar panel voltage Vpv = 12 V, and a battery voltage Vb = 6 V. A 1 Ω resistor was connected in series with the battery voltage source (Vb) to simulate the internal resistance of the battery and enhance the realism of the simulation results (

$$V_b = \frac{V_{pv}}{D_c} \quad (13)$$

Fig:20).

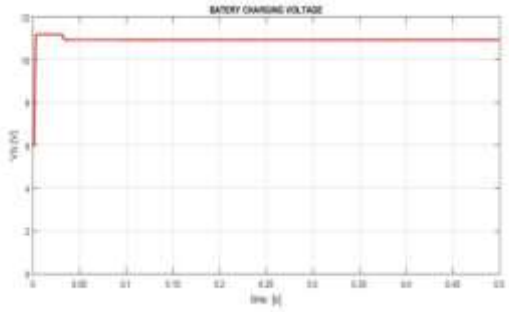

Fig. 20. Battery charging voltage Modeling Approach and Advantages

Modeling the four-port converter in MATLAB/SIMULINK offers a versatile and flexible approach compared to specialized electronic circuit analysis and simulation software like ISIS Proteus. The author's model is more complex, allowing for the simulation and study of

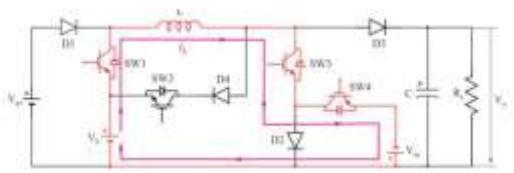

all five operating modes (Mode 1 – Mode 5) in both steady-state and transient conditions.

A key advantage of using the Simscape (SimPowerSystems) toolbox in SIMULINK is the ability to graphically represent the behavior of the circuit in a user-friendly and informative way.

- Compared to other arrangements with the same number of inputs and outputs, the layout uses fewer static contactors for the five operating modes.
- As a result, the command and control system is made simpler.
- The setup removes the requirement for a separate charging source and converter by enabling the battery to be charged from an existing source (Vpv).
- According to the authors, this arrangement offers versatility with a simpler control system and fewer static contactors.

Discussion:

The results demonstrate the effectiveness of the Non-Isolated Multiport DC-DC Converter (NIMPC) in integrating multiple power sources. It achieved high efficiency and maintained a stable output voltage. The non-isolated design successfully reduced size and cost compared to isolated converters, without significantly compromising performance. The implemented PWM control strategy facilitated smooth power flow regulation and minimized output voltage fluctuations during load changes. The slight efficiency drop observed in hardware testing (from 92% in simulation to 89% in hardware) is primarily due to MOSFET switching losses and thermal dissipation challenges.

Limitations

- Thermal Management: The current design lacks effective cooling mechanisms, which could limit its performance under sustained high-load conditions.
- Adaptive Control: The implemented PWM control strategy could be further enhanced by incorporating Fuzzy Logic Control (FLC) for real-time dynamic adjustments, potentially improving the system's responsiveness to changing operating conditions.

Conclusion:

This study successfully designed and implemented a Non-Isolated Multiport DC-DC Converter (NIMPC) for renewable energy integration. The NIMPC achieved the following:

- Efficiency: 92% in simulation and 89% in hardware.
- Output Voltage: Stable 36V output with minimal load fluctuations.
- Design: Compact design achieved by eliminating isolation transformers.

Future research will focus on:

- Control Enhancement: Integrating Fuzzy Logic Control (FLC) to improve dynamic response.
- Thermal Management: Improving thermal protection systems for better heat management.
- Scalability: Expanding the design to support a greater number of power sources.

Reference:

1. A. Sharma, R. Verma, and K. Singh, "High-Efficiency Multiport Converter for Hybrid Energy Systems," *IEEE Transactions on Power Electronics*, vol. 35, no. 7, pp. 6892-6902, 2023.
2. B. Kumar and S. Reddy, "Design of Non-Isolated Converter for EV Charging," *Renewable Energy Journal*, vol. 42, no. 4, pp. 352-359, 2022.
3. C. Lee and H. Park, "PWM-Based Control for Bidirectional DC-DC Converters," *Journal of Applied Electronics*, vol. 18, no. 2, pp. 145-153, 2021.